Novel magnetic core-shell Fe_3O_4 polypyrrole nanoparticles functionalized by peptides or albumin

A. Nan,[a*] R. Turcu,[a] I. Bratu,[a] C. Leostean,[a] O. Chauvet,[b] E. Gautron,[b] and J. Liebscher[c*]

[a]National Institute of Research and Development for Isotopic and Molecular Technologies, Donath 65-103, RO-400293 Cluj-Napoca, Romania
[b]Institute of Materials Jean Rouxel Nantes, 44322 Nantes cedex 3, France
[c]Institute of Chemistry, Humboldt-University Berlin, Brook-Taylor 2, D-12489 Berlin, Germany
E-mail: liebscher@chemie.hu-berlin.de

DOI: http://dx.doi.org/10.3998/ark.5550190.0011.a16

Abstract

Novel magnetic core-shell iron oxide nanoparticles, covered by polypyrrole which is functionalized by covalent attachment of glycyl-leucine or bovine serum albumin were synthesized using *N*-hydroxysuccinimide as activating reagent. The morphology of the functionalized magnetic nanoparticles was investigated by DLS and HRTEM, showing a core-shell structure. The structures of magnetic nanoparticles based on functionalized polypyrrole were investigated by FTIR spectroscopy and X-ray diffraction and the magnetic properties were determined by magnetization measurements.

Keywords: Magnetite, polypyrrole, *N*-hydroxysuccinimide, biomolecules, magnetic nanoparticles

Introduction

Shaping sub-micrometer-sized particles that exhibit more than two different properties, highly desirable for simultaneous and efficient technological applications, can be performed by assembling "building blocks" of several materials into nanocomposites, thereby providing bi-, tri-, or multifunctionality in contrast with their more limited single-component counterparts. Remarkable is therefore the case of nanocomposites with a core/shell structure, which are promising candidates for integrating these multiple, interacting, or independent functionalities. This is accomplished by arrangement of these nanometer-scale building blocks, giving place to superstructures that display various applications such as in medicine,[1] diagnosis,[2] biomedicine,[3-5] in cell separation,[6, 7] in the construction of loudspeaker,[8, 9] as sealing materials,[10, 11] in sink float

separation[12, 13] and in catalysis.[14] It facilitates an understanding of the fundamental rules of their organization.

For many biotechnological and technological applications magnetic nanoparticles are of great interest. Here, functionalisation of their surface is of high relevance. The functions can be directly attached to the magnetic nanoparticles by adsorption or by using polymers, such as polypyrrole (PPy). The latter polymer was found to be biocompatible in vitro and in vivo[15] and increasing interest has evolved for biochemical and medical applications of polypyrroles in general. Here, proteins[16-24] (glycosidase and other enzymes, collagene, fibrinogene, heparine), biotine[25, 26] or polysaccharides[25] were immobilized on PPy films or polymer NP covered with PPy.

Coating with biomolecule-functionalized PPy was recently used to improve the biocompatiblitiy of metallic surfaces in implant material for biomedical application. Fe_3O_4 nanoparticles coated by biofunctionalized polypyrrole are rare. So far, folic acid[27] and the cancer antibody herceptine[28], amino acids[29] and DNA[30] were used to functionalize PPy-Fe_3O_4 nanoparticles. These functions were fixed to the polypyrrole layer of core-shell nanoparticles by formation of an amide bond using the carbodimide method Recently, coating of polystyrene-Fe_3O_4 NP with carboxylate-functionalized PPy was used for covalent fixation of biotin via N-hydroxysuccinate activation.[31]

Here, we report the first examples of PPy-Fe_3O_4 NP with a peptide or bovine serum albumine BSA function. Unlike in the cases of biotin-functionalized magnetic NP reported by Chehimi et al.[31] the core of the PPy coated magnetic NP does consist of Fe_3O_4 NP´s stabilized by fatty acids rather than of Fe_3O_4 which is already covered with a primary polymer shell (polystyrene).

Results and Discussion

Syntheses of monomers and magnetic nanocomposites

3-(Pyrrol-1-yl)propanoic acid as readily available starting material was transformed into the N-hydroxysuccinate **2** with N-hydroxysuccinimide (NHS) and EDC using a reported procedure[24] (Scheme 1).

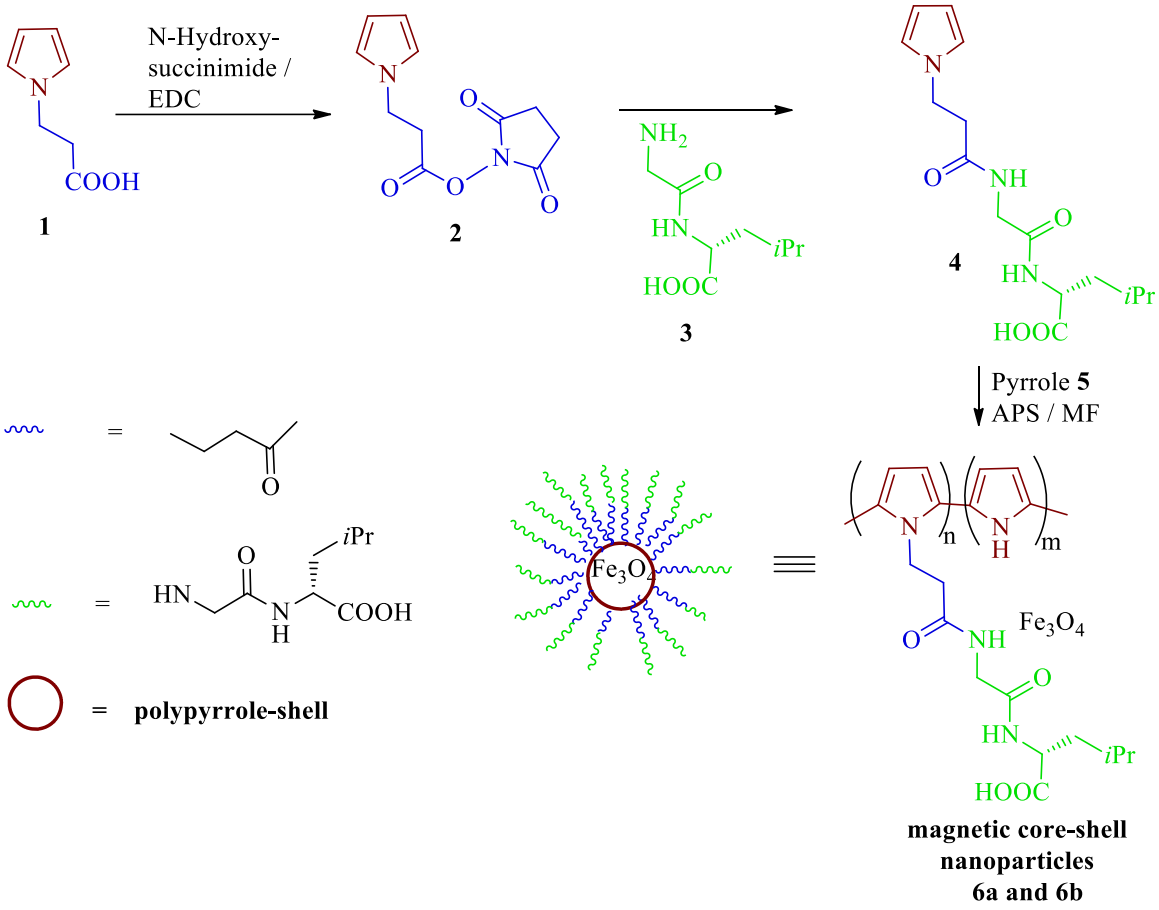

Scheme 1. Synthesis of magnetic core-shell nanoparticles functionalized with H-Gly-Leu-OH moieties.

Condensation of **2** with the unprotected glycyl-leucine (H-Gly-Leu-OH) **3** gave high yields of the pyrrole-containing N-acylation product **4**. This monomer was copolymerized with unsubstituted pyrrole **5** in the presence of Fe_3O_4-magnetic nanofluid (MF) to provide magnetic core-shell nanoparticles **6** covered by a polypyrrole shell, which is functionalized by dipeptide moieties. The copolymerization was carried out in a water/ethanol mixture containing ammonium persulfate (APS) as oxidant and water based MF (Scheme 1). Two ratios of monomers **5** and **4** and two different MF stabilized by double layers of oleic acid (OA) or lauric acid (LA), respectively, were used (see Table 1). Peptide-nanoparticles **6** appeared as black precipitates, which were purified by washing with water/methanol mixtures and isolated by magnetic separation.

Table 1. Synthesis parameters for core-shell-nanoparticles **6** functionalized by Gly-Leu **3**

Sample*	monomer ratio **4** : **5**	MF type
6a	1 : 1	OA+OA
6b	3 : 1	LA+LA

*ratio of MF/(**4** + **5)** = 10:1, ratio of APS/**(4** + **5)** = 1:2

The water based MF were prepared by a known two-stage process[32, 33] starting with co-precipitation of Fe^{3+} and Fe^{2+} in aqueous medium at 80 – 82 °C, followed by the addition of oleic acid, lauric acid or dodecylbenzensulfonic acid (*v. s.*)as surfactant.

Functionalization of surface activated magnetic polypyrrole-core-shell nanoparticles by BSA

The BSA-functionalized magnetic core shell PPy-Fe_3O_4 nanoparticles **9** were synthesized starting from dodecylbenzosulfonate stabilized MF following up another strategy (Scheme 2). 3-(Pyrrol-1-yl)-propanoyl-N-hydroxysuccinate **2** was first oxidatively (APS) copolymerized with unsubstituted pyrrole **5** in a monomer ratio of 3:1 in aqueous solution in the presence of MF. The ratio of MF/pyrrole monomers (**2** : **5)** was 10:1 (v/v) and the ratio of APS/pyrrole monomers (**2** + **5)** 0.5. The resulting, surface-activated PPy-Fe_3O_4 nanoparticles **7** were separated and washed by phosphate-buffered saline solution (PBS, pH 7.4) and then, in the second step, were treated with BSA in the same buffer solution. In this way, BSA substituted a part of the N-hydroxysuccinate groups while the others survived and gave propionic acid moieties by hydrolysis. The resulting BSA-functionalized nanoparticles **9** were purified by repeated washing with buffer solution and water by intermediate magnetic separation.

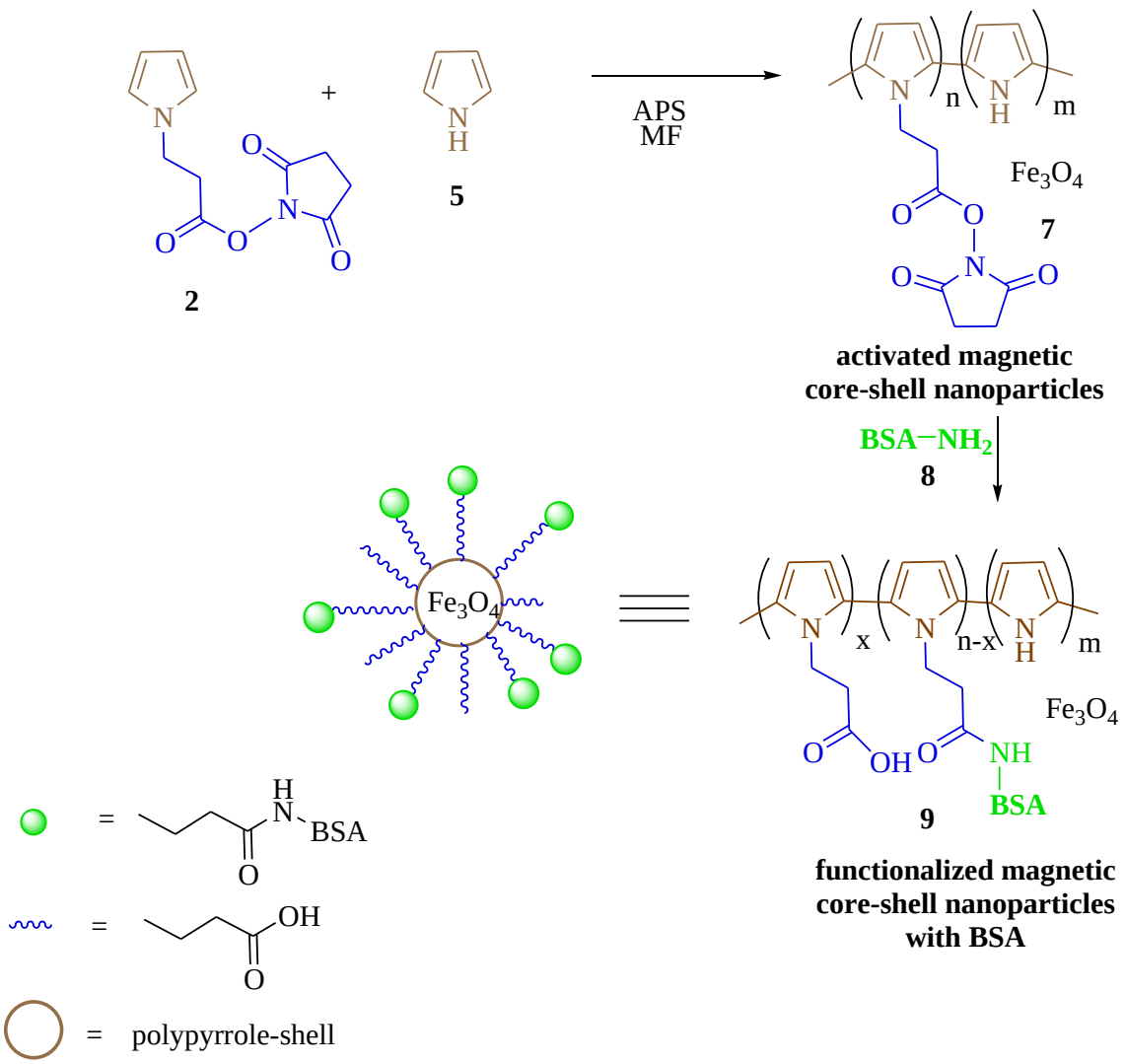

Scheme 2. Synthesis of magnetic core-shell nanoparticles functionalized with BSA.

Morphological characterization

The HRTEM images of functionalized magnetic copolymer nanostructures **6a** and **6b** (see Figure 1) confirm a core-shell structure consisting of Fe_3O_4 crystalline magnetic cores covered by a thin (1.5-3 nm) copolymer shell in these cases. The thickness of the copolymer shells is mainly influenced by the polymerization time. There is also some aggregation seen in the images which is caused by the preparation of the sample by evaporation of the solvent out of a solution.

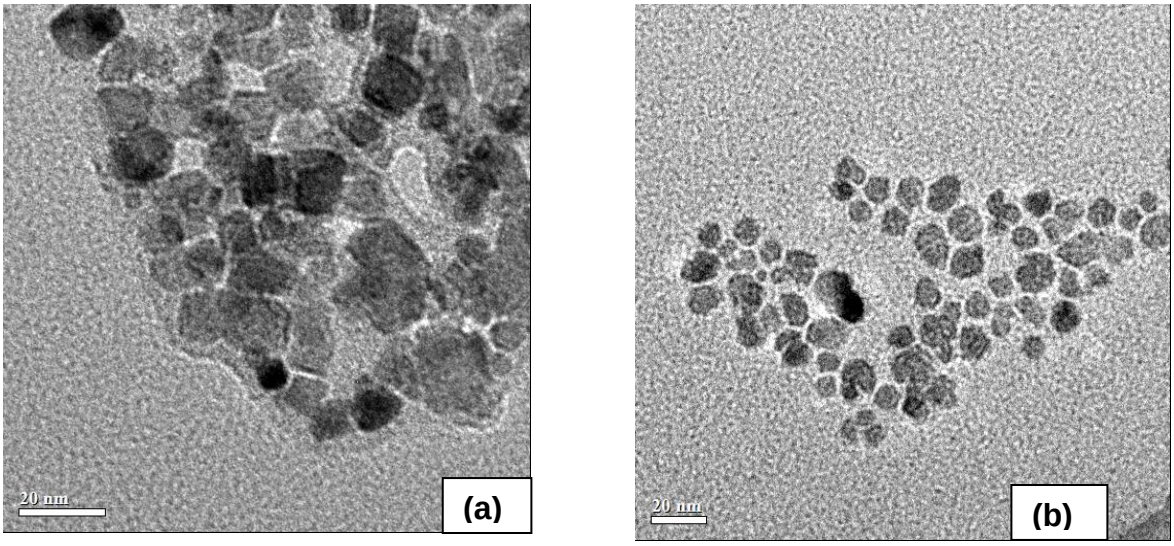

Figure 1. HRTEM images of functionalized magnetic copolymer nanostructures: (a) – **6a**, (b) – **6b.**

Dynamic light scattering experiments of **6a** revealed a hydrodynamic diameter of 93.5 nm, a diffusion coefficient of $4.8080 \cdot 10^{-8}$ and a polydispersion of 0.191. The significantly larger mean hydrodynamic diameter than the mean diameter observed by HRTEM revealed that particle agglomeration must have occurred in water.

X-Ray-diffraction

X-Ray-diffraction was carried with magnetic core-shell NP´s **6b** (see Figure 2b). For comparison, the XRD of the MP´s which are found in the nanofluid stabilized by a double layer of lauric acid (LA + LA) is shown in Figure 2a. The results demonstrate that core-shell nanoparticles **6b** display crystalline Fe_3O_4 structure. The characteristic peaks at 2θ angles correspond very well to the standard card of magnetite PDF-No: 01-071-6337. The background noise and the low intensities observed for **6b** are caused by the amorphous polymeric shell.

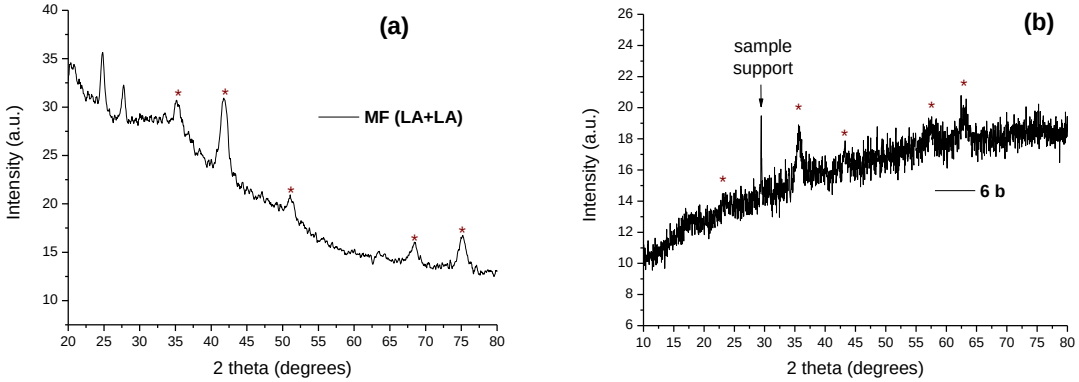

Figure 2. XRD spectra for: (a) MF (LA+LA); (b) magnetic nanoparticles **6b**.

FTIR spectroscopic investigations

FTIR spectra were recorded from all functionalized MP **6a, 6b** and **9** (Figures 3 and 4). For comparison, FTIR-spectra of monomeric Gly-Leu-functionalized pyrrole **4** (Figure 3) as well as of BSA, polypyrrole and activated core-shell-nanoparticle **7** (Figure 4) were included. The latter shows an intense peak at 1741 cm^{-1} for the N-hydroxysuccinate C=O groups. The strong absorption band around 570 cm^{-1} appearing in all functionalized MP´s, is ascribed to Fe_3O_4. A band at 1701 cm^{-1} for amide C=O is found in the monomer **4** as well as in the Gly-Leu-functionalized MP **6a** and **6b.** The spectra of magnetic nanoparticles **6a**, **6b**, **7** and **9** containing functionalized polypyrroles show significant changes of the intensities and peak positions of the typical pyrrole ring vibration bands as compared with polypyrrole PPy. The peaks located at 914, 1190, 1465 cm^{-1} for PPy are shifted to higher wave numbers in the functionalized cases. Furthermore, the absorption bands ascribed to the collective vibration mode of intra-ring and inter-ring C=C/C-C shift from 1550 cm^{-1} in PPy to 1560 cm^{-1} in magnetic nanoparticles **7** and **9** and 1580 cm^{-1} for dipeptide-functionalized nanoparticles **6b**. The position of this band is correlated with the conjugation length of the polymer chain [34], the shift to higher frequencies indicates a decrease of the conjugation length of the copolymer in the functionalized magnetic nanoparticles as compared to PPy.

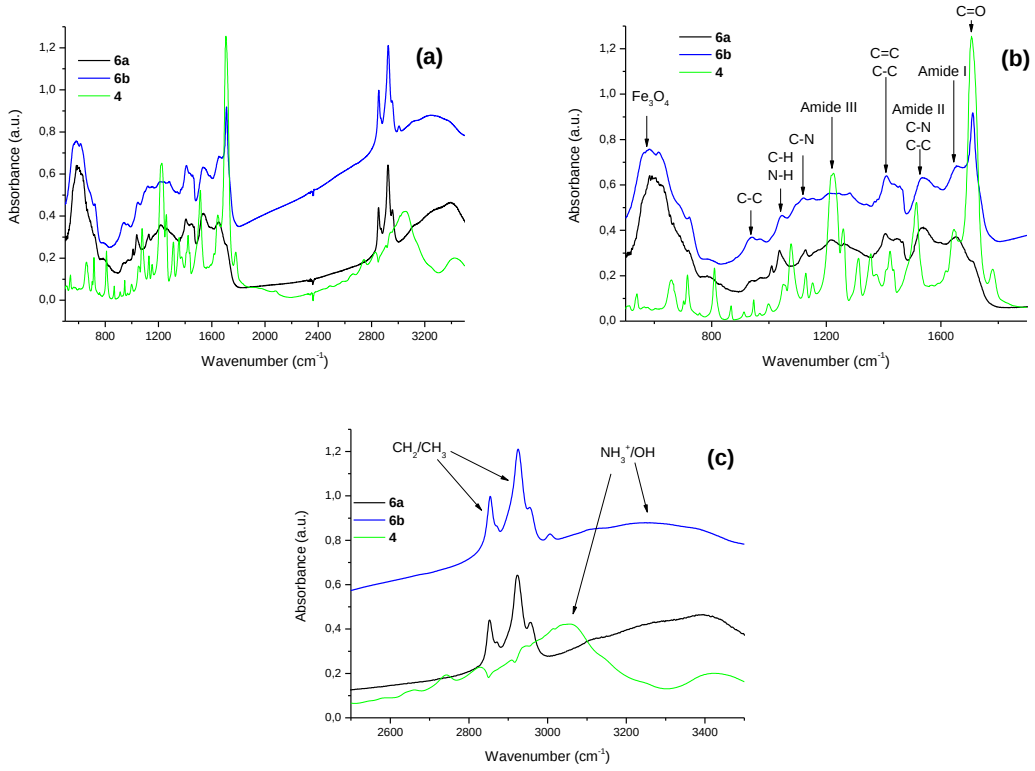

Figure 3. (a) Complete FTIR spectra of magnetic nanoparticles **6a** and **6b** functionalized with dipeptide and spectrum of substituted pyrrole **4**; (b) expanded FTIR spectra 500 – 1900 cm^{-1}; (c) expanded FTIR spectra 2500 – 3500 cm^{-1}.

Concerning the spectrum of BSA (Figure 4), the spectral region of the amide I band (~1656 cm^{-1}) of proteins is due to the in-plain C=O stretching vibration, which weakly couples with C-N stretching and in-plain N-H bending[35]. This band is very sensitive to the secondary structure (i.e. α-helix, β-sheet, β-turns and unordered) and consequently, different C=O stretching frequencies are superimposed if different secondary structures are found in a protein. Thus the position and shape of the amide I band can be used to determine the secondary structure types present in a protein.

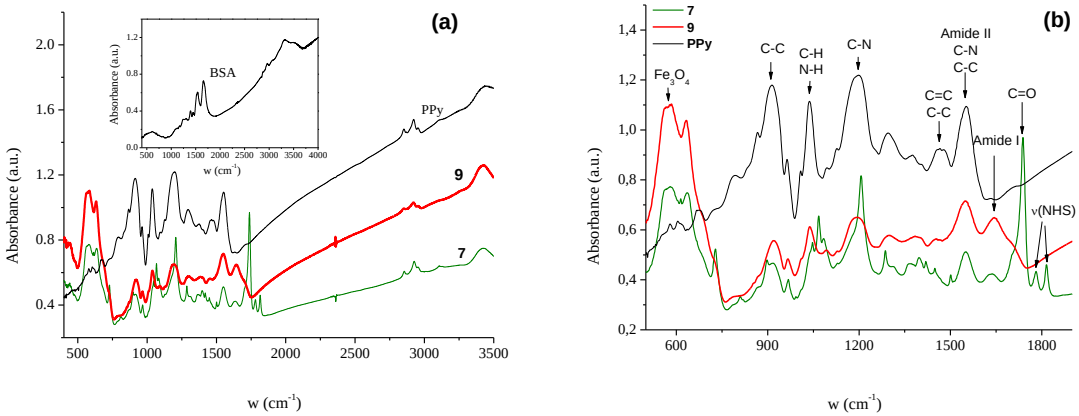

Figure 4. (a) Full FTIR spectra of magnetic nanoparticles of **7** and **9** and the spectrum of **PPy** and **BSA** for comparison; (b) expanded FTIR spectra 500 – 1900 cm^{-1}.

Figure 5 shows the deconvolution of the amide I band of BSA and BSA-functionalized magnetic core-shell nanoparticles **9**, respectively. The results of the deconvolution analysis shown in Table 2 reveal that a change in the secondary structures of BSA occurred in the process of covalent fixation to the magnetic nanoparticle. While ß-sheet content increased by about 50 % the ß-turn amount diminished to about one tenth in the course of the immobilization. The α-helix amount was less affected.

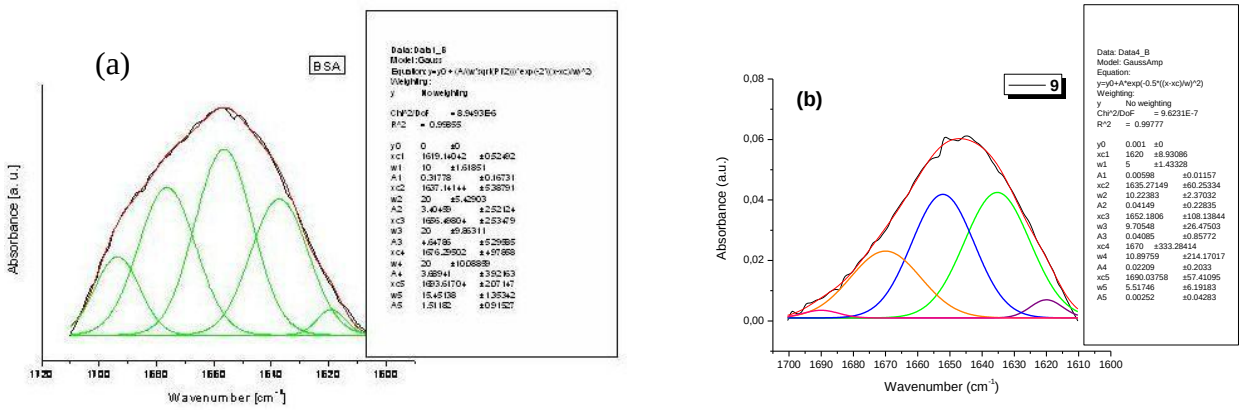

Figure 5. (a) Secondary structure analysis of BSA by amide I band deconvolution; (b) Secondary structure analysis of BSA-functionalized magnetic nanoparticles **9** by amide I band deconvolution.

Table 2. Relative contributions (%) of different secondary structural units of neat BSA and BSA-functionalized magnetic core-shell nanoparticles **9**

Sample	β-sheet	α-helix	β-turn
BSA	25	34	27
9	44	43.8	2.4

Magnetic measurements

Figures 6a and 6b show the behavior of the magnetization at room temperature for functionalized core-shell magnetic-polypyrrole nanostructures **6a**, **6b**, **7** and **9**, respectively. The magnetization curves at room temperature of all investigated samples did not show hysteresis loops, thus proving the superparamagnetic behavior of the particles. For such systems, the magnetic moment of the particle is free to rotate in response to the applied magnetic field when the blocking temperature is exceeded.

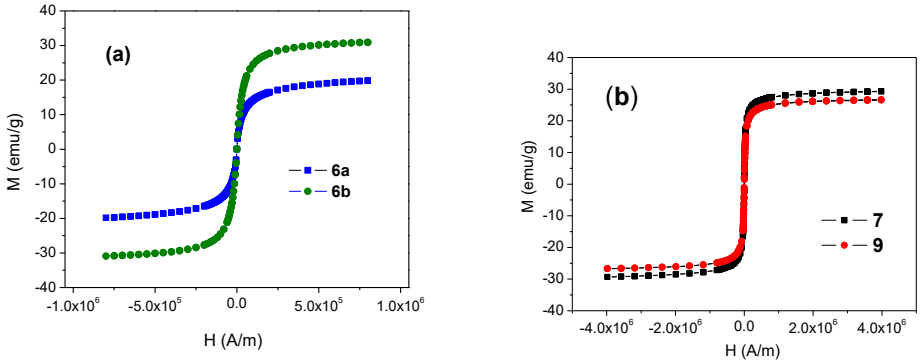

Figure 6. (a) Magnetization vs. applied magnetic field at room temperature of functionalized magnetic nanocomposites **6a** and **6b**; (b) Magnetization vs. applied magnetic field at room temperature of magnetic nanocomposites **7** and **9**.

The measurements show that the synthesis parameters used in the preparation of magnetic core shell nanoparticles, such as the nature of surfactants used for magnetic fluid stabilization and the ratio of unsubstituted pyrrole/substituted pyrrole as well as the functions attached to final MP´s influence the values of saturation of magnetization (M_S) of the nanocomposites.

Conclusions

In summary, we synthesized novel PPy-Fe_3O_4 magnetic core-shell nanoparticles which are functionalized by a covalently linked dipeptide or BSA. The former represents the first example where a peptide was covalently fixed to the PPy-shell of such NP´s. Formation of the functionalized core-shell nanoparticles were proved by HRTEM, DLS, XRD and FTIR. Fixation of BSA affects the secondary structure composition of this protein in such a way that the amount of ß-sheets increased on the expense of ß-turns. The core-shell nanoparticles show superparamagnetic behavior at room temperature, this characteristic is required for their applications in biotechnology and medicine. Because the synthesis is very flexible, it could also be applied to other peptides, in particular to those exhibiting biological recognition functions and to other proteins. Such investigations are currently underway in our laboratories.

Experimental Section

General. Elemental analysis was performed in a LECO CHNS – 932 apparatus. ^{1}H-NMR and ^{13}C-NMR solution spectra were recorded at 300 MHz and 75 MHz, respectively; with a Bruker AC 300 in $CDCl_3$ as the solvent in 5mm NMR tubes with TMS as internal standard. The assignment of ^{13}C signals is based on APT measurements. HRMS was obtained with a Waters UPLC, LCT Premier XE instrument. The morphology of functionalized magnetic nanoparticles based magnetic nanocomposites was determined by HRTEM using Hitachi H9000NAR transmission electron microscopes. XRD were measured with a diffractometer DRON 3M X-ray, working at 35 kV and 35 mA. The Co K_α radiation, Fe filtered was collimated with Soller slits. FT-IR spectra were carried out on a JASCO FTIR 610 spectrophotometer. The magnetic measurements were performed at room temperature using a Vibrating Sample Magnetometer DMS 880. The N-hydroxysuccinate **2** was prepared in analogy to a reported procedure.[24]

Synthesis of (*S*) 2{2-[3-(1H-pyrrol-1-yl)-propanoyloxyamino]acetamido}-4-methylpentanoic acid (4). 2 (0.6 g, 2.54 mmol) and glycyl-leucine **3** (0.47 g, 2.54 mmol) were dissolved in THF (40 ml). After stirring at room temperature for 24 h the white precipitate was filtered off and washed 5 times with distillated water yielding pure product **4**. Yield 75 %, m. p.= 167-169 ºC, ^{1}H-NMR (300 MHz, MeOD): δ = 0.93 (d, *J* = 6.3Hz, 2H), 0.98 (d, *J* = 6.3Hz, 2H), 1.62 (m, 2H), 1.73 (m, 1H), 2.7 (t, *J* = 7.1 Hz, *J* = 14.3 Hz, 2H), 3.88 (d, *J* = 6 Hz, 2H), 4.21 (t, *J* = 6.2 Hz, *J* =

13.6 Hz, 2H), 4.46 (m, 1H), 6.02 (dd overlapped, $J_1 = J_2 = 2.1$ Hz, 2H), 6.68 ppm (dd overlapped, $J_1 = J_2 = 2.1$ Hz, 2H), ^{13}C-NMR (75 MHz, MeOD): δ = 20.4 (-CH_3), 22.0 (-CH_3), 24.6 (-CH-(CH_3)$_2$), 37.9 (-CH_2-), 40.7 (-CH_2-*i*-Pr), 42.5 (-CH_2-), 46.8 (-CH_2-CO-NH), 50.6 (-CH-COOH), 107.6 (-CH, pyrrole ring β positions), 120.1(-CH, pyrrole ring α positions), 170.0 (-C=O), 172.4 (-C=O), 174.5 (-COOH) ppm. $C_{15}H_{23}N_3O_4$ (309.36) calcd.: C 58.24, H 7.49, N 13.58; found: C 58.63, H 7.31, N 13.37. IR (KBr), ν (cm^{-1}): 1708 (s) (C=O), 1642 (w) (Amide I), 1514 (s) (Amide II), 1420 (m) (C=C/C-C), 1224 (s) (Amide III). HRMS (ESI): *m/z* $[M-1]^-$ calcd for $C_{15}H_{22}N_3O_4^-$: 308.1610; found: 308.1619.

Synthesis of 6a. Pyrrole (0.067 ml, 1 mmol), **4** (0.309 g, 1 mmol) and magnetic nanofluid (0.788424 g Fe_3O_4, 12.5 ml) were dissolved in a mixture of distilled water (10 ml) and ethanol (10 ml) and stirred for 30 minutes. APS (0.228 g, 1 mmol) were dissolved in distilled water (5 ml) and added dropwise to the preformed mixture. The reaction proceeded at room temperature under magnetic stirring 20 h. The reaction was terminated by adding excess methanol to the reaction flask. The resulting black precipitate was separated by magnetic separation, washed with water and dried at 60 ^{0}C for 24 h. IR (KBr), ν (cm^{-1}): 2852, 2924 (s) (CH_2/CH_3), 1708 (w) (C=O), 1656 (w) (Amide I), 1533 (m, b) (C-N/C-C), 1401 (m, b) (C=C/C-C), 1036 (s) (C-H/N-H), 583 (s) (Fe_3O_4).

Synthesis of 6b. Pyrrole (0.067 ml, 1 mmol), **4** (0.927 g, 3 mmol) and magnetic nanofluid (0.788424 g Fe_3O_4, 16.07 ml) were dissolved in a mixture of distilled water (10 ml) and ethanol (10 ml) and stirred for 30 minutes. APS (0.228 g, 1 mmol) were dissolved in distilled water (5 ml) and added dropwise to the preformed mixture. The reaction proceeded at room temperature under magnetic stirring 20 h. The reaction was terminated by adding excess methanol to the reaction flask. The resulting black precipitate was separated by magnetic separation, washed with water and dried at 60 ^{0}C for 24 h. IR (KBr), ν (cm^{-1}): 2849, 2921 (s) (CH_2/CH_3), 1708 (s) (C=O), 1654 (w) (Amide I), 1533 (m, b) (C-N/C-C), 1405 (m, b) (C=C/C-C), 1037 (w) (C-H/N-H), 578 (s) (Fe_3O_4).

Synthesis of 6b. Pyrrole (0.067 ml, 1 mmol), **4** (0.927 g, 3 mmol) and magnetic nanofluid (0.788424 g Fe_3O_4, 16.07 ml) were dissolved in a mixture of distilled water (10 ml) and ethanol (10 ml) and stirred for 30 minutes. APS (0.228 g, 1 mmol) were dissolved in distilled water (5 ml) and added dropwise to the preformed mixture. The reaction proceeded at room temperature under magnetic stirring 20 h. The reaction was terminated by adding excess methanol to the reaction flask. The resulting black precipitate was separated by magnetic separation, washed with water and dried at 60 ^{0}C for 24 h. IR (KBr), ν (cm^{-1}): 2849, 2921 (s) (CH_2/CH_3), 1708 (s) (C=O), 1654 (w) (Amide I), 1533 (m, b) (C-N/C-C), 1405 (m, b) (C=C/C-C), 1037 (w) (C-H/N-H), 578 (s) (Fe_3O_4).

Synthesis of 7. Pyrrole (0.067 ml, 1 mmol), **3** (0.7 g, 3 mmol) and magnetic nanofluid (5 ml) were dissolved in distillated water (20 ml) and stirred for 30 minutes. APS (0.456 g, 2 mmol) were dissolved in distilled water (5 ml) and added dropwise to the preformed mixture. The reaction proceeded at room temperature under magnetic stirring 20 h. The reaction was terminated by adding excess methanol to the reaction flask. The resulting black precipitate was

separated by magnetic separation, washed with water and dried at 60 ^{0}C for 24 h. IR (KBr), ν (cm^{-1}): 2851, 2921 (m) (CH_2/CH_3), 1841, 1780 (w) (C=O of N-hydroxysuccinimide group) 1735 (s) (C=O), 1638 (w) (Amide I), 1548 (m, b) (C-N/C-C), 583 (s) (Fe_3O_4).

Synthesis of 9. Nanoparticles **7** (0.45 g) were washed 3 times with phosphate-buffered saline solution (PBS, pH 7.4) (2 ml). BSA (0.020 g) was poured into phosphate-buffered saline solution (1 ml). Both solutions were gentle mixed with a rotator tube RS-60 for 2 h at room temperature. The mixed solution was kept in refrigerator for 24 h and hand stirred from time to time. The resulting BSA-functionalized nanoparticles **9** were purified by repeated washing three times with buffer solution $NaHCO_3$ (pH = 8) and three times with PSB solution and two times with water. The product was kept in solution and analyzed. IR (KBr), ν (cm^{-1}): 2859, 2919 (m) (CH_2/CH_3), 1645 (m, b) (Amide I), 1548 (m,b) (Amide II), 578 (s) (Fe_3O_4).

Acknowledgements

We thank Dr. Alexander Knoll and Dr. Sergej Ovodov, Biogenes Berlin for assistance in the BSA fixation and Dr. Mike Ahrens, Institute of Chemistry, Humboldt-University Berlin for measuring XRD. We greatly acknowledge to Dr. Doina Bica† and Dr. Ladislau Vekas for ferrofluids samples preparation. This work was supported by CNCSIS –UEFISCSU, project number PNII – IDEI code 76/2010, Surface and interface science: physics, chemistry, biology, applications.

References

1. (a) Gao, X.; Cui, Y.; Levenson, R. M.; Chung, L. W. K.; Nie, S. *Nat. Biotechnol*. **2004**, *22*, 969. (b) Michalet, X.; Pinaud, F. F.; Bentolila, L. A.; Tsay, J. M.; Doose, S.; Li, J. J.; Sundaresan, G.; Wu, A. M.; Gambhir, S. S.; Weiss, S. *Science* **2005**, *307*, 538. (c) C. Alexiou, W. Arnold, R. J. Klein, F. G. Parak, P. Hulin, C. Bergemann, W. Erhardt, S. Wagenpfeil, A. S. Lubbe, *Cancer Res.***2000**, *60*, 6641.
2. (a) Rabin, O.; Perez, J. M.; Grimm, J.; Wojtkiewicz, G.; Weissleder, R. *Nat. Mater*. **2006**, *5*, 118. (b) Ferrari, M. *Nat. Rev. Cancer* **2005**, *5*, 161. (c) Whitesides, G. M. *Nat. Biotechnol.* **2003**, *21*, 1161. (d) Medintz, I. L.; Uyeda, H. T.; Goldman, E. R.; Mattoussi, H. *Nat. Mater*.**2005**, *4*, 435.
3. (a) Tartaj, P.; Del Puerto Morales, M.; Veintemillas-Verdaguer, S.; Gonzalez- Carreno, T.; Serna, C. *J. Phys. D: Appl. Phys.* **2003**, *36*, R182. (b) Berry, C. C. *J. Mater. Chem.* **2005**, *15*, 543. (c). Kaufner, L.; Cartier, R.; Wustneck, R.; Fichtner, I.; Pietschmann, S.; Bruhn, H.; Schutt, D.; Thunemann, A. F.; Pison, U. *Nanotechnology* **2007**, *18*, 1. (d) Ceyhan, B.; Alhorn, P.; Lang, C.; Schüler, D. N. *Small* **2006**, *2*, 1251.
4. (a) Lee, C. W.; Huang, K. T.; Wei, P. K.; Yao, Y. D. *J. Magn. Magn. Mater.* **2006**, *304*, e412. (b) Fütterer, C.; Minc, N.; Bormuth, V.; Codarbox, J. H.; Laval, P.; Rossier, J.; Viovy, J. L. *Lab Chip* **2004**, *4*, 351.

5. Wuang, S. C.; Neoh, K. G.; Kang, E. T.; Pack, D. W.; Leckband, D. E. *Adv. Funct. Mat.* **2006**, *16*, 1723.
6. Alexiou, Ch.; Schmid, R.; Jurgons, R.; Bergemann, Ch.; Arnold, W.; Parak, F. G. Targeted tumor therapy with "magnetic drug targeting": Therapeutic efficacy of ferrofluid bound mitoxantrone; S. Odenbach: Heidelberg: Springer Verlag, 2002, pp 233–251.
7. (a) Safarik, I.; Safarikova, M. *Biomagn. Res. Techn.* **2004**, *2*, 7. (b) Hildebrandt, N.; Hermsdorf, D.; Signorell, R.; Schmitz, S. A.; Diederichsena, U. *Arkivoc* **2007,** (*v*), 79.
8. Rehder, J.; Rombach, P.; Hansen, O. *J. Micromech. Microeng.* **2001**, *11*, 334.
9. Cha, H. G.; Kim, Y. H.; Kim, C. W.; Kwon, H. W.; Kang, Y. S. *Curr. App. Phys.* **2007**, *7*, 400.
10. (a) Li, Z. *J. Magn. Magn. Mater.* **2002**, *252*, 327. (b) Meng, Z.; Jibin, Z.; Jianhui, H. *J. Magn. Magn. Mater.* **2006**, *303*, e428. (c) Jibin, Z.; Li, X.; Lu, Y.; Jianhui, M. *J. Magn. Magn. Mater.* **2002**, *252*, 321. (d) Anton, I.; De Sabata, I.; Vekas, L. *J. Magn. Magn. Mater.* **1990**, *85*, 219.
11. Li, D.; Xu, H.; He, X.; Lan, H. *J. Magn. Magn. Mater.* **2005**, *289*, 399.
12. Van Wayenbarg, B. *Filtration & Separation* **2006**, *43*, 43.
13. Svoboda, J. *Phys. Separation in Science and Engineering* **2004**, *13*, 127.
14. (a) Oila, M. J.; Koskinen, A. M.P. *Arkivoc* **2006**, (*xv*), 76. (b) Alonso, F.; Riente, P.; Yus, M. *Arkivoc* **2008,** (iv), 8. (c) Gayet, F.; Marty, J.-D.; Viguerie N. L.-de, *Arkivoc* **2008**, (*xvii*), 61. (d) Zhou, Y.; He, T.; Wang**,** Z.; *Arkivoc* **2008**, (*xiii*), 80.
15. (a) Wang, X. D.; Gu, X. S.; Yuan, C. W.; Chen, S. J.; Zhang, P. Y.; Zhang, T. Y.; Yao, J.; Chen, F.; Chen, G. *J. of Biomed. Mat. Res. Part A* **2004**, *68A*, 411. (b) Schmidt, C. E.; Shastri, V. R.; Vacanti, J. P.; Langer, R. *Proc. Natl. Acad. Sci. U.S.A.* **1997**, *94*, 8948.
16. Ateh, D. D.; Vadgama, P.; Navsaria, H. A. *Tissue Eng.* **2006**, *12*, 645.
17. Tirkes, S.; Toppare, L.; Alkan, S.; Bakir, U.; Onen, A.; Yagci, Y. *Int. J. of Biol. Macromol.* **2002**, *30*, 81.
18. Haddour, N.; Cosnier, S.; Gondran, C. *J. Am. Chem. Soc.* **2005**, *127*, 5752.
19. Ramanavicius, A.; Mostovojus, V.; Kausaite, A.; Lapenaite, I.; Finkelsteinas, A.; Ramanavicius, A. *Biologija* **2006**, *3*, 43.
20. Cosnier, S.; Gondran, C.; Watelet, J. C. *Electroanalysis* **2001**, *13*, 906.
21. Ateh, D. D.; Vadgama, P.; Navsaria, H. A. *Tissue Eng.* **2006**, *12*, 645.
22. (a) Cosnier, S.; Galland, B.; Gondran, C.; Le Pellec, A. *Electroanalysis* **1998**, *10*, 808. (b) Cosnier, S.; Gondran, C. *Analysis* **1999**, *27*, 558.
23. Bousalem, S.; Benabderrahmane, S.; Sang Y. Y. C.; Mangeney, C.; Chehimi, M. M. *J. Mat. Chem.* **2005**, *15*, 3109.
24. Azioune, A.; Slimane, A. B.; Hamou, L. A.; Pleuvy, A.; Chehimi, M. M.; Perruchot, C.; Armes, S. P. *Langmuir* **2004**, *20*, 3350.
25. Bidan, G.; Billon, M.; Galasso, K.; Livache, T.; Mathis, C.; Roget, A.; Torres-Rodriguez, L. M.; Vieil, E. *Appl. Biochem. Biotechnol.* **2000**, *89*, 183.
26. Lopez-Crapez, E.; Livache, T.; Marchand, J.; Grenier, J. *Clin. Chem.* **2001**, *47*, 186.
27. Wuang, S. C.; Neoh, K. G.; Kang, E. T.; Pack, D. W.; Leckband, D. E. *J. Mater. Chem.* **2007**, ***17***, 3354.

28. Zelikin, A.; Shastri V. R.; Langer, R. *J. Org. Chem.* **1999**, *64*, 3379.
29. Nan, A.; Karsten, S.; Craciunescu, I.; Turcu, R.; Vekas, L.; Liebscher, J. *Arkivoc* **2008**, (*xv*), 307.
30. Lellouche, J.-P.; Senthil, G.; Joseph, A.; Buzhansky, L.; Bruce, I.; Bauminger, E. R.; Schlesinger, J. *J. Am. Chem. Soc.* **2005**, *127*, 11998.
31. Mangeney, C.; Fertani, M.; Bousalem, S.; Zhicai, M.; Ammar, S.; Herbst, F.; Beaunier, P.; Elaissari, A.; Chehimi, M. M. *Langmuir* **2007**, *23*, 10940.
32. Bica, D. *RO Patent* 90078, 1985
33. Bica, D.; Vékás, L.; Avdeev, M. V.; Marinică, O.; Socoliuc, V.; Bălăsoiu, M.; Garamus, V. M. *J. Magn. Magn. Mater*. **2007**, 311, 17.
34. Zerbi, G.; Gussoni, M.; Castiglioni, C. In *Conjugated Polymers*; Bredas, J. L.; Silbey R. Eds.; Kluwer Academic Publisher, 1991, pp 435-507.
35. (a) Qing, H.; Yanlin, H.; Fenlin, S.; Zuyi, T. *Spectrochimica Acta Part A* **1996**, *52*, 1795. (b) Serrano, V.; Liu, W.; Franzen, S. *Biophys J*. **2007**, *93*, 2429. (c) Maruyama, T.; Katoh, S.; Nakajima, M.; Nabetani, H.; Abbott, T. P.; Shono, A.; Satoh, K. *J. Membr. Sci.* **2001**, *192*, 201.